Arsenic adsorption and exchange with phosphorus on indium phosphide (001)

C. H. Li,[1] L. Li,[2] D. C. Law,[1] S. B. Visbeck,[1] and R. F. Hicks[1,*]
[1]*Chemical Engineering Department, University of California, Los Angeles, California 90095-1592*
[2]*Department of Physics and Laboratory for Surface Studies, University of Wisconsin, Milwaukee, Wisconsin 53201*

(Received 22 October 2001; published 20 May 2002)

Arsenic adsorption and exchange with phosphorus on indium phosphide (001) have been studied by scanning tunneling microscopy, low-energy electron diffraction, and x-ray photoelectron spectroscopy. The surface phase diagram as a function of temperature has been obtained. At 285 °C, arsenic adsorbs on the InP $\sigma(2\times4)$ surface (P coverage = 0.25 ML), forming a disordered (1×4) with double layers of arsenic (As + P coverage ~ 1.5 ML). At 330 °C, arsenic adsorbs on the $\sigma(2\times4)$, producing a (2×1) structure with a complete monolayer of group-V dimers. By contrast, some phosphorus desorption occurs above 350 °C, allowing arsenic to displace the phosphorus in the top few layers and converting the $\sigma(2\times4)$ to the $\beta2$ and $\alpha2(2\times4)$ reconstructions (As coverage 0.75 and 0.50 ML, respectively). Above 430 °C, arsenic exchange with InP yields an InAs (4×2) reconstruction. Quantitative analysis of the x-ray photoemission spectra has revealed that substitution of arsenic for phosphorus is limited to the top two to three surface bilayers.

DOI: 10.1103/PhysRevB.65.205322 PACS number(s): 68.35.Bs, 68.37.Ef, 81.05.Ea, 81.15.Gh

I. INTRODUCTION

Heterostructures made of III-V compound semiconductors, such as heterojunction bipolar transistors (HBT's), are mostly grown by metalorganic vapor phase epitaxy (MOVPE).[1] During the growth of these heterojunctions, e.g., InGaAs/InP, the group-V sources must be switched from phosphorus to arsenic. It is found that in InGaAs/InP multiple quantum wells grown by MOVPE, there is a strong dependence of interfacial quality on growth sequence, with interfaces in which InGaAs is grown on InP being substantially smoother and more abrupt than those in which InP is grown on InGaAs.[2–4] Hence the group-V exchange reaction between phosphorus and arsenic is a fundamentally important process, because it affects both the interface properties and the uniformity of quantum structures.

The interaction of arsenic with InP (001) surfaces has been studied by several research groups,[5–11] with a consensus being reached that the InAs surface layer stabilizes at around two to three bilayers in thickness, with no significant arsenic incorporation beyond this region.[5–7] In addition, the activation energy of arsenic exchange with phosphorus was determined to be from 1.2 to 1.6 eV.[8–11] However, detailed structural information—for example, the surface phase diagram—has not been provided so far.

In this paper, we present a study of arsenic adsorption and exchange on the InP (001) $\sigma(2\times4)$ reconstruction. The composition and structure of the surface have been determined by scanning tunneling microscopy (STM), low-energy electron diffraction (LEED), and x-ray photoelectron spectroscopy (XPS). We have observed five phases, with decreasing As coverage and increasing surface temperature: a disordered (1×4) and an ordered (2×1), $\beta2(2\times4)$, $\alpha2(2\times4)$, and (4×2). For the latter three phases, the XPS results indicate that arsenic substitutes for phosphorus in the top few bilayers.

II. EXPERIMENTAL METHODS

The samples were prepared by growing indium phosphide films, 0.5 μm thick, on InP (001) substrates in an MOVPE reactor.[12] After growth, the samples were transferred directly into an ultrahigh-vacuum (UHV) cluster tool with a base pressure of 2.0×10^{-10} Torr, via a turbo-pumped interface chamber. Details of this system have been described elsewhere.[12] The InP (001) crystals were annealed at 673 K for 15 min to obtain a clean and well-ordered indium-rich $\sigma(2\times4)$ reconstruction,[13] and this was verified by low-energy electron diffraction and scanning tunneling microscopy.

Arsenic from two different precursors—arsine (AsH_3) and tertiarybutylarsine (TBAs)—was introduced into the chamber at 1×10^{-5} Torr (unless otherwise specified) through a leak valve for 5–200 min [3.0×10^3–1.2×10^5 L, ($1\ L=10^{-6}$ Torr · s)] at temperatures ranging from 250 to 450 °C. Since both precursors produce the same phases with comparable dosages, for the rest of the paper, we will only refer to the arsine (AsH_3) source.

The surface reconstruction after As adsorption was determined by a Princeton Instruments low-energy electron diffractometer. In addition, As $2p$, As $3d$, P $2p$, and In $3d$ core-level x-ray photoelectron spectra were collected with a PHI 3057 spectrometer equipped with a concentric hemispherical analyzer, multichannel detector, OMNI-III lens with variable acceptance angle, and Al $K\alpha$ x-ray source. The As $2p$ and $3d$ spectra were collected to determine the relative distribution of arsenic atoms in the surface and lower layers, since the mean free path of the $2p$ photoelectrons is much smaller than that of the $3d$ photoelectrons.[14] All XPS spectra were taken with small area mode with a 7° acceptance angle and 23.5 eV pass energy. A 55° takeoff angle with respect to the surface normal was used. Scanning tunneling micrographs were obtained using a Park Autoprobe/VP scanning tunneling microscope. Tunneling

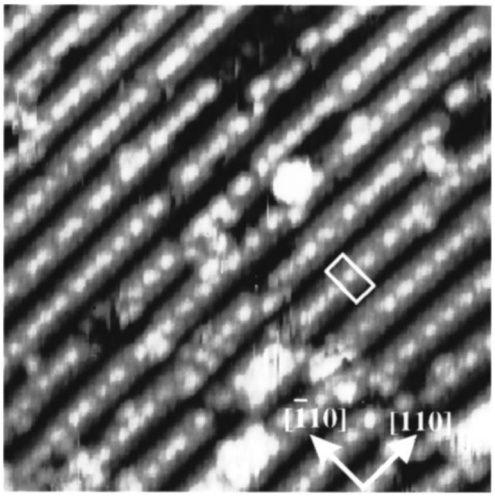

FIG. 1. Scanning tunneling micrograph of the InP (001) $\sigma(2\times4)$ reconstruction: image size$=170\times170$ Å^2 and sample bias$=-3.6$ V.

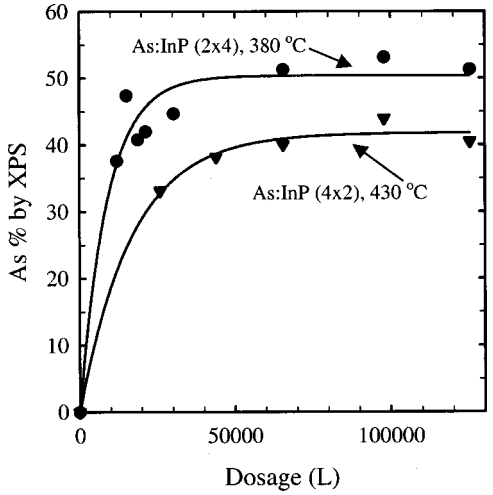

FIG. 2. Saturation coverage of arsenic for the As:InP (2×4) and (4×2) determined by XPS, using the As $2p$ peak area.

was out of filled states with a sample bias of -2.5 to -4.5 V and a tunneling current of 0.5 to 1.0 nA.[12]

III. RESULTS

A. InP (001) $\sigma(2\times4)$ surface

A scanning tunneling micrograph of the InP (001) $\sigma(2\times4)$ surface is shown in Fig. 1. This surface exhibits gray rows extending several hundred angstroms along the [110] axis. In the image, an individual unit cell is highlighted with a white rectangle. It consists of an oblong white spot sitting between a gray ledge and a black trench on either side. The bright spot in the center of the row is due to the filled dangling bonds of a phosphorus dimer. According to the model proposed in previous studies,[13,15,16] the $\sigma(2\times4)$ consists of a single phosphorus dimer straddling four indium dimers, with a P coverage of 0.25 ML. Although theoretical studies predict that this phase is not the most stable In-rich surface, this does not preclude its existence over a specific range of conditions.[15,16] In our studies, the $\sigma(2\times4)$ is observed mixed in with the (2×1) and $\delta(2\times4)$ phases when the phosphorus coverage lies between 1.0 and 0.125 ML.[13] A maximum of about 80% of the surface may be covered with the $\sigma(2\times4)$ at $0.4<\theta_P<0.2$. Presumably, the presence of the other reconstructions helps to stabilize the σ phase.

B. Composition of the surface phases

Dosing arsine onto the $\sigma(2\times4)$ at 285, 330, 380, and 430 °C produces a disordered (1×4) and ordered (2×1), (2×4), and (4×2) reconstructions, as indicated by LEED and STM. Shown in Fig. 2 is the arsenic composition [As (%)] of the (2×4) and (4×2) phases during dosing at elevated temperatures. These values were determined by monitoring the As $2p$ core-level peaks by XPS. The amount of arsenic rises rapidly during AsH_3 exposure, then levels off at about 42% and 52% for the (2×4) and (4×2), respectively. The As uptake for the $d(1\times4)$ and (2×1) is not shown, since in these cases it takes only 5000 L to reach saturation.

Shown in Table I are the atomic compositions of the $d(1\times4)$, (2×1), (2×4), and (4×2) reconstructions. The arsenic percentages calculated using the As $2p$ core-level peaks range from 35.1% to 51.3%. These values are much greater than that calculated using the $3d$ peaks, which range from 10.1% to 17.8%. This suggests that arsenic is confined to a thin surface layer, instead of being distributed evenly throughout the film (see discussion below). In addition, both

TABLE I. Atomic concentration in the near-surface region recorded for different As:InP (001) surface reconstructions.

Reaction temperature	Reconstruction	XPS atomic percentage (using As $2p$ peak)			XPS atomic percentage (using As $3d$ peak)		
		As (%)	P (%)	In (%)	As (%)	P (%)	In (%)
Starting Surface	$\sigma(2\times4)$	0	37.2	62.2	0	37.2	62.2
285 °C	$d(1\times4)$	38.6	25.6	35.8	13.0	29.3	57.7
330 °C	(2×1)	35.1	24.2	40.7	10.1	33.5	56.4
380 °C	(2×4)	51.3	13.9	34.8	17.8	23.5	58.7
430 °C	(4×2)	40.0	18.3	41.7	13.8	25.1	61.1

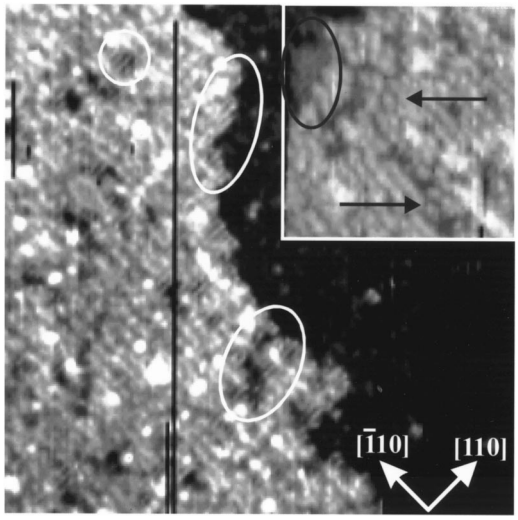

FIG. 3. Scanning tunneling micrograph of the As:InP disordered (1×4) reconstruction: image size$=540\times540$ Å^2, inset$=225\times225$ Å^2, and sample bias$=-3.2$ V.

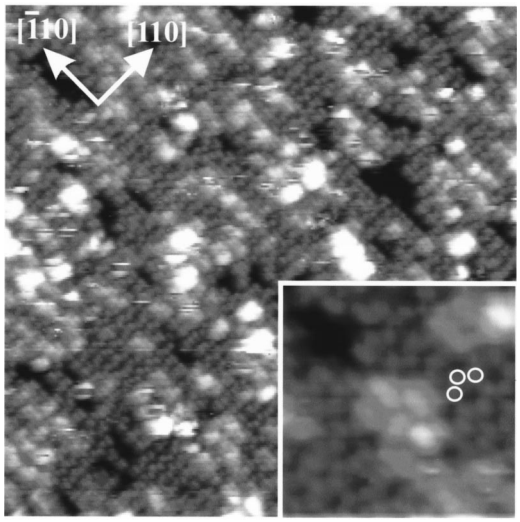

FIG. 4. Scanning tunneling micrograph of the As:InP (2×1) reconstruction: image size$=433\times433$ Å^2, inset$=160\times160$ Å^2, and sample bias$=-3.8$ V.

measurements of the arsenic content show the same trend: that the (2×4) surface contained the most As, followed by the (4×2), $d(1\times4)$, and, last, the (2×1) phase.

C. Surface phase transition

Dosing arsine on the InP (001) $\sigma(2\times4)$ at 285 °C and 5×10^{-5} Torr produces a surface with a weak (2×1) LEED pattern. A filled-states STM image of this surface is shown in Fig. 3. Light gray rows are seen extending in the [$\bar{1}$10] direction and spaced 16 Å apart, yielding a disordered (1×4) structure. Some of these rows are more clearly shown in the inset in Fig. 3. They are not well ordered and are broken in many places (two examples are indicated by the arrows in the inset). Close examination of the images reveals that there are also dimer rows extending in the opposite direction near the pits and step edges. Several examples are circled in the image and inset. These rows are separated by 8 Å and are most likely responsible for the (2×1) pattern seen in LEED. The vertical distance between the $d(1\times4)$ and (2×1) surfaces is about 1.5 Å or one atomic layer. Note that the former phase occupies more than 90% of the surface area.

After dosing the $\sigma(2\times4)$ with arsine at 330 °C, a much clearer (2×1) LEED pattern is observed. Shown in Fig. 4 is a filled-states STM image of this reconstruction. Inspection of the image reveals that the surface is terminated with rows of buckled dimers oriented along the [110] direction. The distances between adjacent rows are 8 Å, yielding a $2\times$ periodicity. The inset in Fig. 4(b) shows a higher-resolution image of the buckled dimer rows. This reconstruction is analogous to the InP (001)-(2×1), which is terminated with 1.0 ML of phosphorus.[17]

In the image in Fig. 4, one sees many bright white features scattered over the surface. One of these features is shown in the inset. It is elongated in the [$\bar{1}$10] direction and is about 1.5 Å in height. This suggests that the white spots are due to additional arsenic atoms on top of the (2×1), analogous to the disordered rows observed in Fig. 3. However, in Fig. 3, the coverage of the second layer of arsenic atoms is much greater, close to 90%, compared to only 20% for the (2×1) reconstruction shown in Fig. 4.

Dosing AsH_3 at temperatures ranging from 360 to 410 °C produces a sharp $(2\times4)/c(2\times8)$ LEED pattern. A filled-states STM image of this structure is shown in Fig. 5(a). The surface exhibits straight dimer rows that are parallel to the [$\bar{1}$10] crystal axis. The average separation between trenches is 16 Å. This structure is the same as that observed on InAs and GaAs (001) surfaces.[18–20] A closer examination of the STM image reveals that most rows contain two arsenic dimers, as indicated by the black arrows in the picture. However, about 20% of the unit cells consist of only one arsenic dimer, as indicated by white arrows. Figure 5(b) shows a line scan across two double-dimer-unit cells (*AB* in the picture). The profile exhibits saddle-shaped dimer features and symmetric trenches that are at about 2.6 Å in depth, characteristic of the $\beta2(2\times4)$ structure.[19,20] Figure 5(c) is a line scan across two single-dimer-unit cells (*CD* in the picture). In contrast, this profile exhibits a shoulder about 1.4 Å lower than the dimer feature, as well as a trench about 2.8 Å in depth. This line shape is indicative of the $\alpha2(2\times4)$ structure.[18–20]

Exposing the $\sigma(2\times4)$ to arsine at temperatures above 430 °C yields a (4×2) reconstruction, as indicated by LEED. Figure 6 presents a filled-states scanning tunneling micrograph of this surface. Straight gray rows are seen oriented in the [110] direction and laterally separated by 16 Å. In between, these rows are dark stripes that are partially filled with light gray spots. These spots repeat every 8 Å ($2\times$ periodicity). This structure is analogous to the InAs (4×2) prepared by molecular beam epitaxy (MBE),[21] except that in the latter case, the dark stripes are completely filled with the gray spots. Some As-rich (2×4) islands are present on the

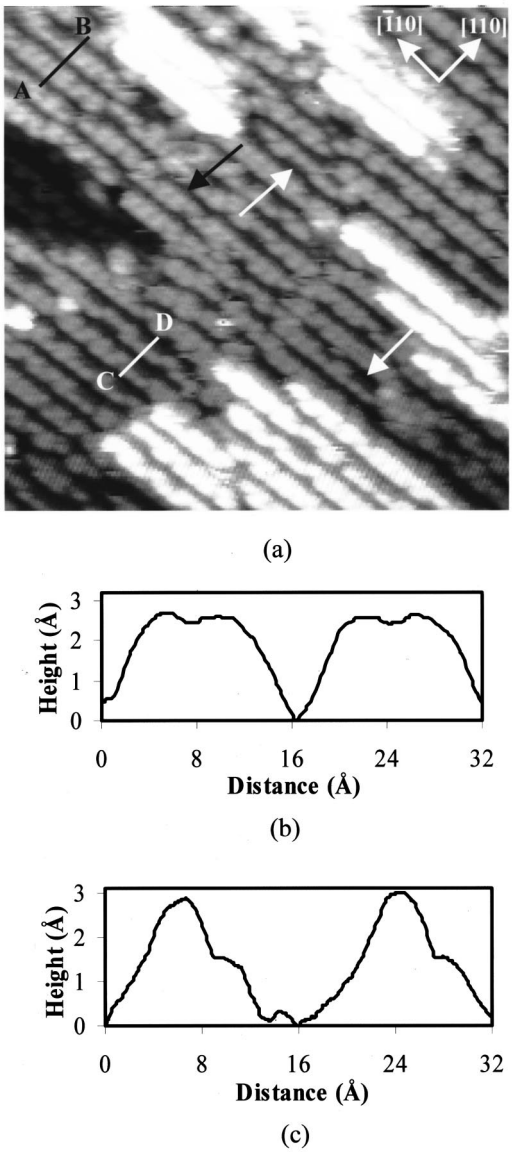

FIG. 5. (a) Scanning tunneling micrograph of the As:InP (2×4) reconstruction: image size=350×350 Å^2 and sample bias =−3.6 V. (b) and (c) Line scans across the image at *AB* and *CD*, respectively.

surface (indicated by the white arrow in the figure). These islands can be removed by further annealing of the sample.

We have performed experiments to check if the phase transition is reversible. Starting from the InAs (4×2) reconstruction and dosing arsenic at temperatures between 360 and 410 °C returns the surface to a (2×4) structure, the same as that observed in Fig. 5. Evidently, this part of the phase diagram is reversible. However, dosing the InAs (2×4) surface with arsine at 330 °C does not produce a (2×1) reconstruction. Instead, the (2×4) LEED pattern remains unchanged. Figure 7 presents an STM picture of a surface prepared in this way. It is covered with straight double-dimer rows extending in the [$\bar{1}$10] direction. Examination of the image reveals the initial formation of (2×1) domains with dimer rows oriented along the [110] crystal

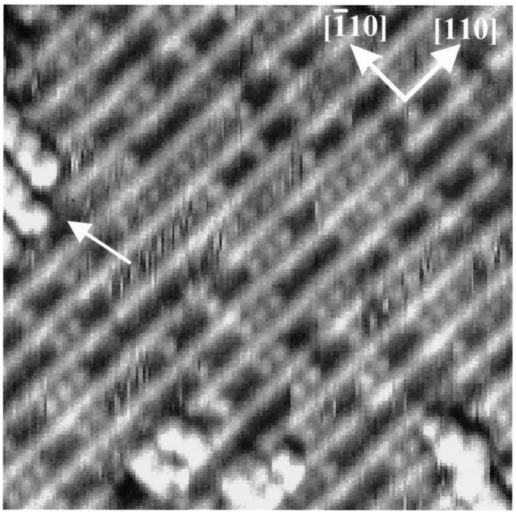

FIG. 6. Scanning tunneling micrograph of the As:InP (4×2): image size=310×310 Å^2 and sample bias=−3.2 V.

axis. Several of these regions are highlighted with black oblong circles in the figure. These domains are one to six rows wide and less than 50 Å in length. Line scans show that they have the same height as the neighboring (2×4) surface.

In Fig. 7, one can see small islands that have nucleated on top of the (2×4) structure. Some of these are demarcated with white boxes in the STM image. The dimer rows contained in these islands are disordered and discontinuous. Line scans indicate that these structures are 4.4 Å or three atomic layers, higher than the underlying (2×4) reconstruction. This suggests that the islands are composed of double layers of arsenic atoms, like the $d(1\times4)$ structure discussed above. Pits of bilayer depth are found near these regions, yielding a surface roughness of 7.3 Å from the top of the island to the bottom of the pit. The surface roughening observed here has also been recorded for the phase transition between the (2×4) and $c(4\times4)$ reconstructions of GaAs (001).[22]

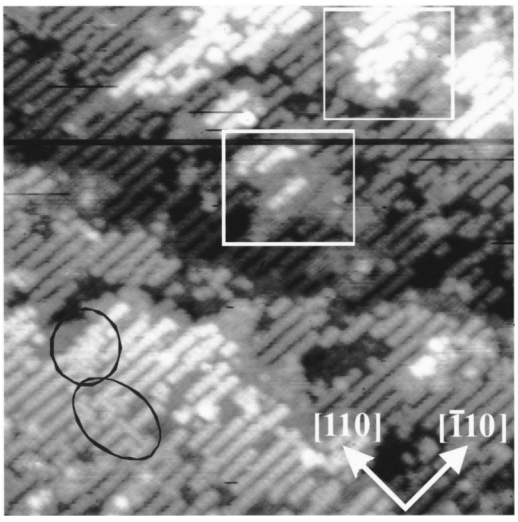

FIG. 7. Scanning tunneling micrograph of the surface after dosing arsenic at 330 °C on the As:InP (2×4) surface: image size =541×541 Å^2 and sample bias=−3.2 V.

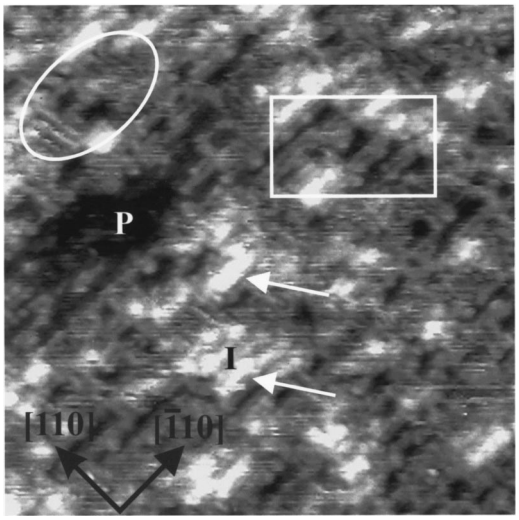

FIG. 8. Scanning tunneling micrograph of the surface after dosing arsenic at 285 °C on the As:InP (2×4): image size=325 $\times$325 Å^2 and sample bias=$-$3.2 V.

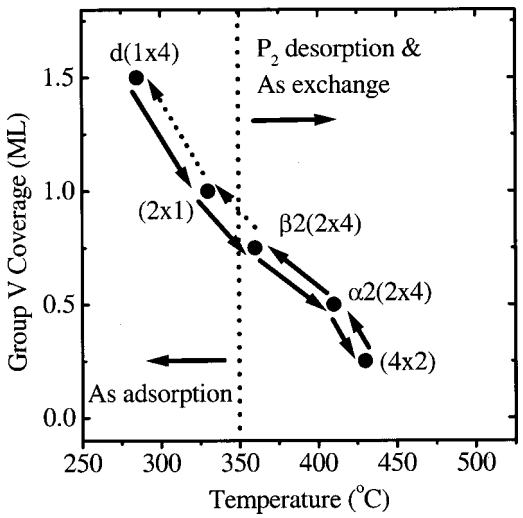

FIG. 9. Surface phases of arsenic adsorbed and exchanged with phosphorous on InP (001) as a function of group-V coverage and temperature.

When the InAs (2×4) surface is dosed with arsine at 285 °C, a weak (2×1) LEED pattern is detected. As shown in Fig. 8, this surface is quite disordered, covered with pits that are two atomic layers deep (marked by ''P'') and islands two atomic layers high (marked by ''I''). In addition, one sees small domains of different reconstructions, as illustrated by rows traversing in the [110] and [$\bar{1}$10] directions. The rows parallel to the [110] axis are 8 Å apart, indicative of a (2×1) structure, while the rows parallel to the [$\bar{1}$10] axis are 16 Å apart, indicative of a (2×4) structure.

IV. DISCUSSION

A. InAs film thickness

The XPS results in Table I indicate that the fraction of arsenic recorded in the near-surface region depends on whether the As $2p$ or $3d$ photoelectrons are used in the calculation of the atomic composition. The reason for this is that the escape depths of the photoelectrons from the two levels are not the same. The As $2p$ binding energy is 1322 eV, so that the photoelectrons leave the surface with a kinetic energy of about 160 eV. This corresponds to a mean free path of ~6 Å (Refs. 5 and 14) or four atomic layers of the film. On the other hand, the As $3d$ binding energy is 44 eV, so that the photoelectrons have a residual kinetic energy of 1440 eV and an escape depth of ~25 Å.[14] The fact that the As concentration saturates at the same arsine dosage, regardless of the core level used in the calculation, suggests that arsenic adsorption and exchange do not extend more than 6 Å below the surface. This finding is in good agreement with previous studies of arsenic adsorption on InP (001).[6,7]

The indium arsenide overlayer thickness T may be estimated from the P $2p$/In $3d$ peak intensity ratios using a model published in the literature.[6,7] This model assumes a uniform in-depth excitation and an exponential decay in the intensity of the photoemission with escape length L that depends only on the kinetic energy. The XPS peak ratio is given by

$$\frac{(\mathrm{P}\ 2p/\mathrm{In}\ 3d)\ \text{in InAs/InP}}{(\mathrm{P}\ 2p/\mathrm{In}\ 3d)\ \text{in InP}} = e^{-T/L(P)}. \qquad (1)$$

For the InP $\sigma(2\times4)$, the P $2p$/In $3d$ peak ratio is 0.60, whereas for the InAs/InP (4×2), the P $2p$/In $3d$ peak ratio is 0.44. The escape length of phosphorus, $L(P)$, equals 18 Å according to Refs. 6 and 23. Therefore, from Eq. (1), the thickness of the indium arsenide layer on top of indium phosphide is 5.6 Å. Similarly, the P $2p$/In $3d$ peak ratio for the InAs/InP (2×4) is 0.40, yielding a layer thickness of 7.3 Å. This is about one atomic layer thicker than that estimated for the (4×2), presumably because the former phase is terminated with 0.75–0.50 ML of arsenic. Note that the above calculation cannot be made for the $d(1\times4)$ and (2×1) structures, because an InAs ''skin'' has not formed on these surfaces.

B. Surface phase transitions

In Fig. 9, the surface phases of adsorbed and exchanged arsenic on indium phosphide (001) are shown as a function of the coverage of group-V elements and the temperature. This phase diagram can be divided into two regimes: below and above the onset of phosphorus desorption at 350 °C. Below this temperature, it is proposed that arsenic adsorbs on the $\sigma(2\times4)$, forming a $d(1\times4)$ or (2×1) reconstruction. Whereas above this temperature arsenic exchanges with phosphorus in the first two to three bilayers, forming a $\beta2(2\times4)$, $\alpha2(2\times4)$, or (4×2) reconstruction. The corresponding As+P coverages on these five phases decline progressively from 1.5 to 1.0 to 0.75 to 0.5 and to ~0.25 ML, respectively. The atomic structure and composition of each of these phases are described next.

Presented in Fig. 10 is a model illustrating the conversion of the InP $\sigma(2\times4)$ into the As:InP (2×1). The $\sigma(2\times4)$

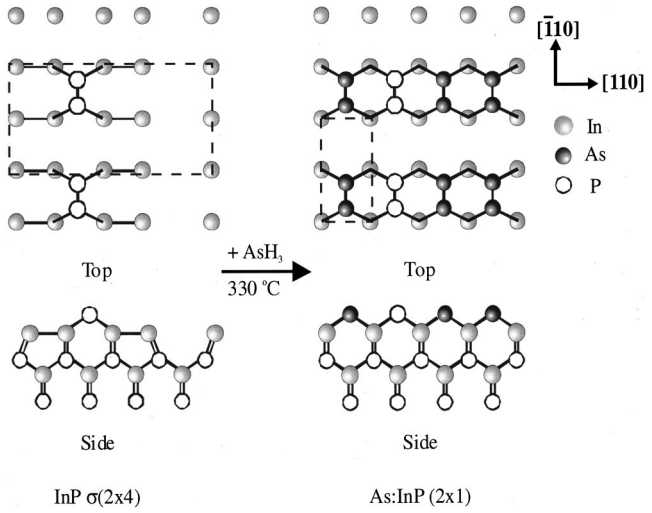

FIG. 10. Ball-and-stick model of the conversion from the $\sigma(2\times4)$ to the (2×1).

unit cell contains one phosphorus dimer bonded to four indium dimers. At 330 °C, arsine decomposes on the surface, depositing three arsenic dimers on top of the indium without displacing the phosphorus atoms. This phase transition is analogous to that observed on InP (001), where the $\sigma(2\times4)$ is converted into the (2×1) by exposure to phosphine below 350 °C.[24,25] We have found that dosing the InP (001)-(2×1) with AsH_3 at 330 °C results in less than 3% As adsorption, confirming that the arsenic cannot displace the phosphorus in this temperature regime. This is consistent with previous studies showing that the As-P exchange reaction is an activated process (E_a equal to 1.2 –1.6 eV), requiring temperatures in excess of 350 °C to proceed at an appreciable rate.[8–11]

At an even lower temperature of 285 °C, additional arsenic adsorbs on the InP surface, forming the disordered (1×4) reconstruction. A ball-and-stick model of this structure is proposed in Fig. 11. It consists of half a monolayer of arsenic dimers deposited on top of the (2×1) surface. The As dimer rows are separated by 16 Å, yielding the $(\times4)$ periodicity observed in the STM picture (Fig. 3). The arsenic dimers in the next lower layer are randomly distributed in the area between the rows, producing a $(1\times)$ pattern that is consistent with the LEED and STM results. Although not shown in the model, the As dimer rows resting on top of the arsenic layer are discontinuous and misaligned with each other, further contributing to the disorder.

Arsenic exchange with phosphorus at 360–410 °C produces the $\beta2(2\times4)$ and $\alpha2(2\times4)$ reconstructions. Models of these two structures are presented in Fig. 12. They are essentially the same as those reported for the As-rich InAs (001) surface.[18,26,27] The $\beta2(2\times4)$ is terminated with two As dimers in the top layer and one As dimer in the trench. On the other hand, the $\alpha2(2\times4)$ consists of one As dimer in the first and third layers, separated by two indium dimers in the second layer. These models are in good agreement with the STM image and line scans shown in Fig. 5. In keeping with the XPS results, arsenic is substituted for phosphorus in the first three bilayers of the crystal.

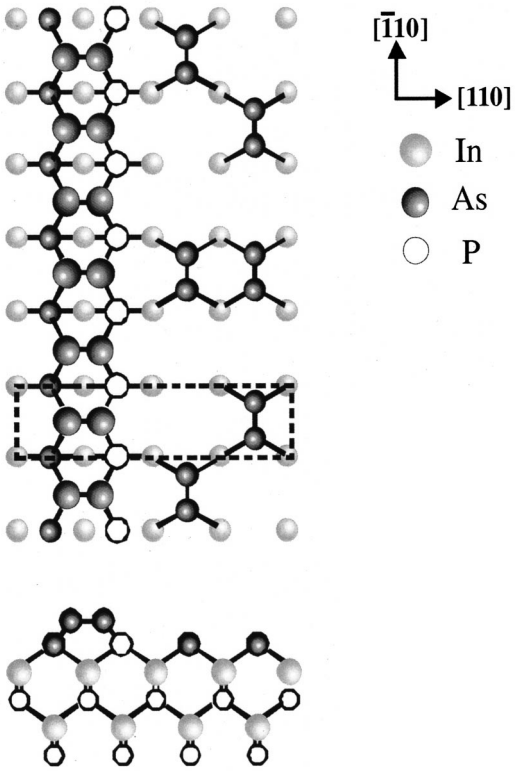

FIG. 11. Ball-and-stick model of the $d(1\times4)$ reconstruction.

At or above 430 °C, arsenic exchange with phosphorus on indium phosphide (001) generates the (4×2) reconstruction. The atomic structure of InAs (4×2) has been studied by theoretical and experimental means, and several models have been proposed.[21,28–32] These include two indium dimers in the top layer followed by one in the trench,[28] one indium dimer in the first layer and two in the trench,[29–31] and two indium dimers in the top layer with two second-layer arsenic dimers.[21] However, which of these best represents the atomic structure of this surface is still being debated and further research is needed to resolve this issue. Nevertheless, the STM image shown in Fig. 6 is identical to that seen for the InAs (001) (4×2) (Refs. 21 and 31) and demonstrates that an indium arsenide film has been deposited on the indium phosphide substrate by exposure to arsine at 430 °C.

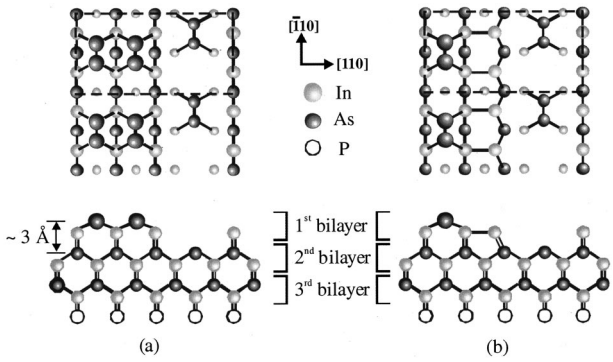

FIG. 12. Ball-and-stick models of the (a) $\beta2(2\times4)$ and (b) $\alpha2(2\times4)$ reconstruction.

Once the InAs skin has formed on top of the InP crystal, the $d(1\times4)$ and (2×1) reconstructions observed at lower temperatures can no longer be obtained. Instead, the deposition of additional arsenic yields a rough surface morphology as shown in Figs. 7 and 8. These surfaces are covered with small domains of the (2×1) and (2×4) phases, and with additional islands having structures intermediate between the $c(4\times4)$ and (2×4) reconstructions found on InAs and GaAs (001).[18,22]

V. CONCLUSIONS

In summary, we have identified the phase diagram for arsenic adsorption and exchange on InP (001) during exposure to 1×10^{-5} Torr arsine, or tertiarybutylarsine, at 250–450 °C. Below the phosphorus desorption temperature ~350 °C, arsenic adsorbs on top of the $\sigma(2\times4)$ surface, forming either a $d(1\times4)$ or a (2×1) with 1.5 or 1.0 ML of As and P atoms. Above the phosphorus desorption temperature, arsenic exchanges with phosphorus in the first three bilayers, forming an InAs film ~7.3 Å thick. In this case, three reconstructions are observed at progressively higher temperatures: the $\beta2(2\times4)$, $\alpha2(2\times4)$, and (4×2) with As coverages of 0.75, 0.50, and ~0.25 ML, respectively.

ACKNOWLEDGMENTS

Funding for this research was provided by the National Science Foundation, Divisions of Chemical and Transport Systems and Materials Research.

*Author to whom correspondence should be addressed. Electronic address: rhicks@ucla.edu

[1] G. B. Stringfellow, *Organometallic Vapor-Phase Epitaxy: Theory and Practice* (Academic, San Diego, CA, 1999).
[2] A. Y. Lew, C. H. Yan, R. B. Welstand, J. T. Zhu, C. W. Tu, E. T. Yu, and P. K. L. Yu, J. Electron. Mater. **26**, 64 (1997).
[3] S. L. Zuo, W. G. Bi, C. W. Tu, and E. T. Yu, Appl. Phys. Lett. **72**, 2135 (1998).
[4] S. L. Zuo, W. G. Bi, C. W. Tu, and E. T. Yu, J. Vac. Sci. Technol. B **16**, 2395 (1998).
[5] G. Hollinger, D. Gallet, M. Gendry, C. Santinelli, and P. Viktorovitch, J. Vac. Sci. Technol. B **8**, 832 (1990) and references within.
[6] J. M. Moison, M. Bensoussan, and F. Houzay, Phys. Rev. B **34**, 2018 (1986).
[7] J. M. Moison, C. Guille, M. Van Rompay, F. Barthe, F. Houzay, and M. Bensoussan, Phys. Rev. B **39**, 1772 (1989).
[8] H. Ikeda, Y. Miura, N. Takahashi, A. Koukitu, and H. Seki, Appl. Surf. Sci. **82**, 257 (1994).
[9] Z. Sobiesierski, D. I. Westwood, P. J. Parbrook, K. B. Ozanyan, M. Hopkinson, and C. R. Whitehouse, Appl. Phys. Lett. **70**, 1423 (1997).
[10] J. Jönsson, F. Reinhardt, K. Ploska, M. Zorn, W. Richter, and J.-Th. Zettler, in *Proceedings of the Sixth International Conference on Indium Phosphide and Related Materials* (IEEE, New York, 1994), p. 53.
[11] N. Kobayashi and Y. Kobayashi, J. Cryst. Growth **124**, 525 (1992).
[12] L. Li, B.-K. Han, S. Gan, H. Qi, and R. F. Hicks, Surf. Sci. **398**, 386 (1998).
[13] L. Li, Q. Fu, C. H. Li, B.-K. Han, and R. F. Hicks, Phys. Rev. B **61**, 10 223 (2000).
[14] S. Tanuma, C. J. Powell, and D. R. Penn, Acta Phys. Pol. A **81**, 169 (1992).
[15] W. G. Schmidt, F. Bechstedt, N. Esser, M. Pristovsek, Ch. Schultz, and W. Richter, Phys. Rev. B **57**, 14 596 (1998).
[16] N. Esser, W. G. Schmidt, J. Bernholc, A. M. Frisch, P. Vogt, M. Zorn, M. Pristovsek, W. Richter, F. Bechstedt, Th. Hannappel, and S. Visbeck, J. Vac. Sci. Technol. B **17**, 1691 (1999).
[17] L. Li, B.-K. Han, Q. Fu, and R. F. Hicks, Phys. Rev. Lett. **82**, 1879 (1998).
[18] C. Ratsch, W. Barvosa-Carter, F. Grosse, J. H. G. Owen, and J. J. Zinck, Phys. Rev. B **62**, R7719 (2000).
[19] T. Hashizume, Q. K. Xue, J. Zhou, A. Ichimiya, and T. Sakurai, Phys. Rev. Lett. **73**, 2208 (1994).
[20] T. Hashizume, Q. K. Xue, A. Ichimiya, and T. Sakurai, Phys. Rev. B **51**, 4200 (1995).
[21] Q. K. Xue, Y. Hasegawa, T. Ogino, H. Klyama, and T. Sakurai, J. Vac. Sci. Technol. B **15**, 1270 (1997).
[22] M. J. Begarney, L. Li, C. H. Li, D. C. Law, Q. Fu, and R. F. Hicks, Phys. Rev. B **62**, 8092 (2000).
[23] P. Cheng, D. Bolmont, and C. A. Sebenne, J. Phys. C **15**, 6101 (1982).
[24] M. J. Begarney, C. H. Li, D. C. Law, S. B. Visbeck, Y. Sun, and R. F. Hicks, Appl. Phys. Lett. **78**, 55 (2001).
[25] Y. Sun, D. C. Law, S. B. Visbeck, and R. F. Hicks (unpublished).
[26] H. Yamaguchi and Y. Horikoshi, Jpn. J. Appl. Phys., Part 2 **33**, L1423 (1994).
[27] H. Yamaguchi and Y. Horikoshi, Phys. Rev. B **48**, 2807 (1993).
[28] D. K. Biegelsen, R. D. Bringans, J. E. Northrup, and L.-E. Swartx, Phys. Rev. B **41**, 5701 (1990).
[29] S. Ohkouchi and N. Ikoma, Jpn. J. Appl. Phys., Part 1 **33**, 3710 (1994).
[30] N. Ikoma and S. Ohkouchi, Jpn. J. Appl. Phys., Part 1 **34**, 5763 (1995).
[31] C. Kendrick, G. LeLay, and A. Kahn, Phys. Rev. B **54**, 17 877 (1996).
[32] C. Kumpf, D. Smilgies, E. Landemark, M. Nielsen, R. Feidenhans'l, O. Bunk, J. H. Zeysing, Y. Su, R. F. Johnson, L. Cao, J. Zegenhagen, B. O. Fimland, L. D. Marks, and D. Ellis, Phys. Rev. B **64**, 075307 (2001).